THERMAL/HYDRAULIC BOWING STABILITY ANALYSIS OF GRID-SUPPORTED MULTI-PIN BUNDLES WITH DIFFERENTIAL SWELLING AND IRRADIATION CREEP

G. McAREAVEY

United Kingdom Atomic Energy Authority, Reactor Group, Risley, Warrington, WA3 6AT, United Kingdom

SUMMARY

Azimuthal variations of clad temperature in fuel pin bundles lead to pin bowing by differential thermal expansion. During irradiation in a fast flux further possibly more severe bowing is caused by differential neutron induced voidage swelling, which, being temperature sensitive, will also vary azimuthally.

Bowing tends to enhance clad diametral temperature differences, the convex side becoming hotter and the concave side cooler. Thus there is a positive feed-back from heat transfer which may lead to bowing instability, due to differential expansion at the start of life, or, for initially stable conditions, due to the combined effects of thermal expansion and irradiation swelling. Swelling may decrease with temperature at high temperature giving either positive or negative feed back according to axial location.

Accompanying irradiation induced swelling is the phenomenon of irradiation induced creep, which will reduce clad bending stresses, and may influence distorted pin shapes.

The problem of pin bowing in a fuel element cluster thus involves consideration of the thermal/hydraulic behaviour, allowing for both inherent and induced clad temperature non-uniformities, coupled with the restrained bowing behaviour, including differential thermal expansion, differential swelling, and irradiation creep. All pins must be considered simultaneously. In the temperature and stress ranges of interest thermal creep may be neglected.

An existing computer code, IAMBIC, the basis of which was described in SMIRT-3 paper D 1/7, solves the zero time thermal bowing problem for a cluster of up to 61 pins on hexagonal pitch, with up to 21 supports at arbitrary axial spacing, allowing for the effect on coolant flow distribution of the irregular geometry of peripheral sub-channels and the continuously distorted pin shapes. Pin displacements in perpendicular planes due to input random transverse displacements at the support points are calculated and passed to the thermal/hydraulic routine which calculates axial and azimuthal variation of clad temperature. New pin shapes are calculated including thermal bowing, and the iterative cycle is repeated to convergence or excessive bow.

The time dependent features can be introduced by equating the total axial strain rate at azimuthal position θ to the sum of the elastic, thermal expansion, swelling and irradiation creep strain rates. From this the equation for the time rate of change of pin curvature at axial position z and time t is developed.

The time integration of this equation requires a knowledge of the variation of swelling with neutron dose at varying temperature, information which is not usually available, since swelling data are normally accumulated at constant temperature. Two possibilities are considered:

(a) the swelling rate at the current neutron dose and temperature equals the isothermal rate for that dose and temperature

(b) the swelling rate at the current neutron dose and temperature equals the isothermal rate for that dose and the initial temperature.

With these assumptions the axial variation of curvature at time t can be determined, The subsequent iterative procedure for determining bowed pin shapes and associated clad temperatures follows the IAMBIC pattern. The analysis is embodied in a computer code called TRIAMBIC.

1. INTRODUCTION

Current designs of LMFBR fuel element sub-assemblies comprise large bundles of closely pitched slender pins. To maintain uniformity of coolant flow distribution and to inhibit fluid-induced vibrations, structural supports in the form of grids or spirally-wound wires are employed. The pins can thus be considered as slender beams with multiple restraints.

Azimuthal non-uniformities of clad temperature arise due to both systematic and random departures from ideal conditions. Systematic effects are associated with transverse power gradients due to the reactor radial flux gradients or proximity to control rods, and non-uniform distribution of sub-channel coolant flow at the edge of the bundle. Random non-uniformities arise from dimensional tolerances on pins, support grids or wire-wraps, and wrappers (Fig 1).

The first harmonic components in transverse perpendicular directions of the clad azimuthal temperature variations give rise instantaneously to thermal bowing through differential thermal expansion. Multi-point supports generally cause the bow to alternate in direction in adjacent spans. Where the bowing acts to reduce the sub-channel area on the hotter side of the pin the temperature difference in that direction will increase. There is thus a tendency for successive increments of temperature difference to cause successive increments of bow in the same direction, a process which may be limited only by pin contact, leading to overheating and possibly premature clad failure.

During irradiation in a fast flux cladding materials experience a progressive growth due to the development of voids within the lattice structure [1]. Since voidage growth in stainless steels is strongly temperature dependent [2], transverse temperature gradients causing differential axial growth will lead to further bowing. Once again each increment of bow will be amplified through its interaction with the coolant flow distribution, causing enhanced differential thermal expansion and a potentially higher rate of differential voidage growth.

At high neutron dose the pseudo-expansion coefficient of voidage swelling ($\partial \epsilon_{sw}/\partial T$) for a typical stainless steel cladding may be many times greater than the thermal expansion coefficient, and has a large axial variation. The bowing problem thus increases considerably as irradiation proceeds, and an initially stable configuration could become unstable.

Bending stresses induced by the restraints will be subject to relaxation by irradiation creep, and at the higher temperatures by thermal creep. In the highest dose regions, where neutron induced voidage bowing is likely to be most severe, clad temperatures are relatively low and irradiation creep will be dominant. In the present analysis thermal creep is neglected.

The aim is to provide a method by which the number and spacing of pin supports may be optimised to maintain adequate pin spacing at minimum cost to neutron economy and parasitic pressure loss. Such a method should therefore include the following features:

a) hydraulic analysis to determine coolant flow distribution
b) thermal analysis to evaluate coolant and clad temperature distribution
c) flexure analysis for statically indeterminate beams
d) provision for initially bowed pins

e) provision for mis-alignment of support points

f) allowance for axial thrust

g) allowance for grid/pin clearance designed to accommodate irradiation-induced pin distension

h) allowance for compliance of pin supports

i) calculation of differential neutron voidage growth

j) thermal and irradiation creep relaxation effects

k) feed-back between the thermal/hydraulic behaviour and the bending analysis.

Such a comprehensive analysis has not yet been attempted. However, the general problem has been tackled in a number of different ways, with varying degrees of approximation.

2. CURRENT STATUS

The time dependent pin bowing problem combines complex thermal hydraulics analysis with inelastic analysis of statically indeterminate beams. Numerous purely thermal hydraulic codes of varying complexity have been developed and those capable of dealing with more than a few pins are invariably of the sub-channel type. Of these SABRE [3] and COBRA-III [4] are among the more complex and can also include initially bowed pins. THI-3D [5] also incorporates axial variation of flow area. No structural analysis is included in any of these.

The BOBL code [6] developed at Petten, principally to evaluate the effect of pin bowing behind blockages on the flow and temperature fields, appears to be limited to four inter-connected sub-channels of different shape. The sub-channel thermal hydraulic model is relatively complex and the equations are solved iteratively in conjunction with equations for elastic thermal bowing of slender pins. Grid supports in one plane are assumed, but there is a facility for generating further supports where pins bow to touch. Reasonably good agreement between predictions and experimental results is found both for pin bowing and temperatures [7]. It is also claimed that elastic theory is quite adequate to predict the results of experiments in which plastic deformation occurs. Differential neutron voidage swelling is not considered.

An analysis by US workers applied to a peripheral pin of a grid-supported sub-assembly consisted of iterating between a complex finite element code for creep analysis of statically indeterminate beams, CRASIB [8], and a thermal hydraulic code. CRASIB considers one pin at a time, and it is not clear whether sympathetic bowing of neighbouring pins is included in the analysis. Irradiation creep and voidage swelling are included.

Bowing of pins in thermal reactors has been considered by Veeder and Schankula [9], and Merckx [10], the former concentrating on pellet/clad interaction effects and the latter on axial thrust with spring restraints at grid supports (using an extension of CRASIB called AXIBOW). In LMFBRs voidage growth of the clad tends to limit pellet/clad interaction, and neutron flux differentials across individual pins are small. However, if pins became jammed in grids axial thrust could be important, and since this problem may be solved by compliant grids, spring restraints would need to be modelled.

Cornet and Capart [11] used an approximate method to determine a bowing stability criterion for peripheral pins with both thermal and neutron voidage bowing feedback.

In the present study the approach has been to simplify the thermal hydraulic model so as to enable a fairly large pin bundle (up to 61 pins) with random grid cell mis-alignment (up to 21 grids), edge channel over-cooling, and transverse power gradients to be simulated. As with BOBL the thermal and mechanical aspects are combined in a single code working iteratively. The IAMBIC code [12] was designed for elastically restrained thermal bowing only, but as shown later it can be adapted to calculate neutron voidage bowing under certain conditions. TRIAMBIC, the basis of which is described herein, is a time dependent code which includes irradiation creep, differential voidage growth, initial pin bow, and flow re-distribution due to wrapper wall dilation. Results are not yet available from this code.

3. THEORETICAL MODEL FOR THE TRIAMBIC CODE

The bowing of each pin in a cluster influences the neighbouring pins by disturbing the coolant flow distribution, and hence the temperature distribution, in the common sub-channels. Thus neighbouring pins will bow, influencing their neighbours in turn. Clearly one must consider the behaviour of all the pins simultaneously in order to take account of the mutual interactions.

This is accomplished in the thermal hydraulic model of the TRIAMBIC code. The model is essentially the same as that used in IAMBIC [see ref 12] except that the limitations to deflections small compared with the pin/pin gaps are removed.

3.1 Coolant flow distribution

In common with most fuel element cluster thermal hydraulic analyses TRIAMBIC uses the sub-channel approximation in which coolant velocities and temperatures are regarded as uniform over the cross-section of a sub-channel. (Sub-channel configurations are shown in Fig 2.) Sub-channels at the wrapper boundary and in the corners differ in shape, size and equivalent diameter from the rest and usually carry a different mass flow per unit of heated pin surface. For fully developed conditions the nominal distribution of flow between sub-channels can be found from experiments using more convenient fluids (eg Betts et al. [13]) or by use of the equivalent diameter concept. It should be noted, however, that the latter concept may be unsatisfactory for sub-channels of considerably different shape owing to fluid shear at the interfaces and more importantly to secondary flow [14]. For wire-wrap supports the concept leads to large errors and a constant velocity for sub-channels of all types is closer to experimental findings [15].

When sub-channel areas vary axially cross-flows are generated (in addition to those induced by wire-wraps). Ideally axial and transverse momentum equations must be solved simultaneously for each sub-channel as a boundary value problem. The solution of these non-linear equations can present formidable computational difficulties, and some approximation is necessary.

In the present work, to enable a large cluster of interacting pins to be considered, the very simple device of assuming relative axial flow in a sub-channel to be proportional to a power of the local relative sub-channel area was adopted. Comparisons with more elaborate calculations and experimental results using bowed pins show reasonably good agreement. Cross-flows between sub-channels are found from continuity, with the further assumption that at each calculation step the transverse flows associated with each pin should sum to zero.

3.2 Coolant and clad temperatures

Axial conduction of heat is neglected. The heat flux is assumed to be uniform at the fuel periphery, an approximation which is good for oxide fuel but pessimistic for fuel of higher thermal conductivity. Linear heat rating may vary axially and also from pin-to-pin. Allowance is made for peripheral conduction in the cladding, thermal conduction and eddy mixing between coolant sub-channels, and for heat transported by transverse coolant flows generated by the pin bowing and by wire-wraps if present. Implicit in this last effect is the assumption that coolant transferred from one sub-channel to a neighbouring one over a calculation step is uniformly mixed with the coolant already there. Since mixing requires a development length to be effective the assumption is far from self-evident. Experimental work on wire-wrapped clusters appears to support it, but it has not been substantiated for continuously bowing pins with grid supports.

Convective heat transfer in liquid metals is extremely good, and clad temperature distribution normally follows coolant temperature distribution very closely. Dwyer [16] found a marked reduction in circumferentially averaged heat transfer coefficient for a liquid-metal-cooled pin uniformly displaced relative to its neighbours. On the other hand calculations by Hofmann [17] show that when the developing thermal field is allowed for no significant change in mean heat transfer coefficient occurs over a length of 1 m with typical LMFBR fuel pin parameters. In the current work the local heat transfer coefficient is assumed to be a function of the local sub-channel Peclet number and the local ratio of mean pin pitch to pin diameter ratio, using the theoretical results of Pfann [18] modified for very small p/d by the experimental results of Marchese [19]. Calculated pin bow is found to be relatively insensitive to variants from this procedure. The major effect on local average clad temperature stems from changes in local axial gradient of coolant temperature, with little contribution from changes in heat transfer coefficient.

Closely-pitched pins on triangular pitch have been shown both experimentally (Zhukov [20]) and theoretically (Nijsing [21]) to develop a sixth harmonic component of clad temperature variation. This also is largely a reflection of coolant temperature variation from the narrowest to widest pin gaps, which requires a significant axial length to develop. Application of Marchese's [19] experimental results to typical LMFBR fuel pin parameters and a p/d ratio of unity suggests that the amplitude of the fully developed sixth harmonic variation could be $\pm$ 70°C, but the associated development length may be 60 to 100 times the sub-channel equivalent diameter [22]. For very slightly larger p/d ratio and some intra-channel mixing due to wire wraps or grid type spacers Marchese [20] also finds experimentally that the circumferential variation is virtually eliminated. This component of azimuthal clad temperature variation has no relevance to bowing as such but could strongly influence pin endurance. It is not specifically included in TRIAMBIC.

3.3 Irradiation creep distortion of the wrapper walls

Significant bending stresses occur in the flat walls of the hexagonal wrapper due to the internal coolant pressure. These produce irradiation creep deformations giving rise to a complex pattern of dilation in response to axial variation of pressure difference and irradiation dose. Peripheral sub-channel areas, and hence relative coolant flows, are particularly sensitive to these distortions, and the impact on cross-pin temperature

gradients of peripheral pins will be considerable.

Since irradiation creep is relatively insensitive to temperature [23] there is little feed-back on dilation from thermal hydraulics. Thus wrapper distortions can be calculated independently. TRIAMBIC uses such calculations to define the 'nominal' relative flow distribution in edge sub-channels as a function of axial position.

3.4 Thermal hydraulic equations

With the assumptions outlined above the sub-channel coolant temperatures are found by integrating the set of equations (McAreavey [12]):

$$(m_{in} - \sum_{1}^{N} w_j/2)\frac{dT_c}{dz} = \frac{q}{6}\sum^{abc} \phi + \frac{C_p}{\Delta z}\sum_{1}^{N} w_j\,[(1-\beta_j)T_c - \alpha_j T_j] - \eta(3T_c - \sum_{1}^{N} T_{cj})$$

$$- \gamma\{2\Delta T_s \sum^{abc} \phi - \Delta T_{s1}(\phi_a+\phi_b) - \Delta T_{s2}(\phi_b+\phi_c) - \Delta T_{s3}(\phi_c+\phi_a)\} \qquad (1)$$

where ϕ allows for variation of heat rating between pins, α_j and β_j = 0 and 1 respectively for outward flow and the reverse for inward flow, subscripts a, b, and c refer to the three pins bordering the sub-channel, and subscripts 1, 2 and 3 refer to the neighbouring sub-channels,

$$\gamma = 3k_s t/\pi a \qquad \text{and} \qquad \eta = (2\gamma + \sqrt{3}k_e b/p) \qquad (2)$$

At the wrapper boundary allowance can also be made for loss (or gain) of heat to an external by-pass flow of specified temperature distribution, although heat transfer between adjacent sub-assemblies is not included.

Having calculated the coolant temperature distribution the clad temperature averaged over the clad thickness and 60° sectors are found from:

$$T_s - T_c = \phi\,\Delta T_{sj}$$

$$\text{where} \quad \Delta T_s = \frac{q}{\pi}\left\{\frac{1}{h(d+2t)} + \frac{\ell n(1+t/d)}{4k_s}\right\} \qquad (3)$$

3.5 Pin bowing equations

In developing the bowing equations the usual assumptions for bending of slender beams are made:

plane and normal sections remain plane and normal after bending,

displacements are small compared with span length and pin diameter,

shear deflections may be neglected,

irradiation creep is the same for tension as for compression,

bending occurs in perpendicular planes independently.

In addition it is assumed that irradiation creep rate is directly proportional to stress, that the fuel does not contribute to bending stiffness, and that the voidage swelling rate is independent of stress. Then:

$$\dot{\epsilon} = \dot{\epsilon}_e + \dot{\epsilon}_c + \dot{\epsilon}_{sw} + \dot{\epsilon}_{th} \qquad (4)$$

from which:

$$-\zeta\frac{\partial^2 \dot{y}}{\partial z^2}(z,t) = \frac{\dot{\sigma}}{E}(\zeta,z,t) + \beta(\zeta,z)\,\sigma(\zeta,z,t) + \dot{\epsilon}_{sw}(\zeta,z,t) + \alpha_{th}(\zeta,z)\,\dot{T}(\zeta,z,t) \qquad (5)$$

where $(\dot{\cdot})$ indicates time derivative.

Over the temperature range of interest the thermal expansion coefficient α_{th} and Young's modulus E change by less than 10% and 13% respectively and are assumed constant. The variation of irradiation creep rate with temperature is not well established, but is unlikely to be very great. In the present study it is allowed to vary from span to span but not azimuthally.

Writing the azimuthal variation of the clad temperature distribution and the swelling rate as:

$$T = \sum_{n=o}^{\infty} T_n \cos n\theta \tag{6}$$

$$\dot{\epsilon}_{sw} = \sum_{n=o}^{\infty} \dot{S}_n \cos n\theta \tag{7}$$

multiplying through eq (5) by the moment about the neutral axis of an element of clad cross-sectional area $\zeta a t d\theta$ and integrating between limits of θ and 2π, after dividing through by the second moment of area $I = \pi a^3 t$ we have:

$$\frac{\partial^2 \dot{y}(z,t)}{\partial z^2} = \frac{\dot{M}(z,t)}{EI} + \frac{\beta(z)\, M(z,t)}{I} - \frac{\dot{S}_1(z,t)}{a} - \frac{\alpha_{th}\, \dot{T}_1(z,t)}{a} \tag{8}$$

Integrating with respect to time:

$$\frac{\partial^2 y(z,t)}{\partial z^2} - \frac{\partial^2 y(z,o)}{\partial z^2} = \frac{M(z,t)}{EI} - \frac{M(z,o)}{EI} + \frac{\beta(z)}{I} \int_o^t M(z,t)dt$$

$$- \frac{1}{a} \int_o^t \dot{S}_1(z,t) - \frac{\alpha_{th}}{a} \{T_1(z,t) - T_1(z,o)\} \tag{9}$$

But:

$$\frac{\partial^2 y(z,o)}{\partial z^2} = \frac{M(z,o)}{EI} - \frac{\alpha_{th}\, T_1(z,o)}{a} + \frac{d^2 y_o(z)}{dz^2} \tag{10}$$

hence:

$$\frac{\partial^2 y(z,t)}{\partial z^2} = \frac{M(z,t)}{EI} + \frac{\beta(z)}{I} \int_o^t M(z,t)dt - \int_o^t \frac{\dot{S}_1(z,t)}{a} dt - \frac{\alpha_{th}\, T_1(z,t)}{a} + \frac{d^2 y_o(z)}{dz^2} \tag{11}$$

where $y_o(z)$ is initial bow, which may be expressed as a series of polynomials in z.

In the absence of thermal creep the time scale can be read as a scale of neutron dose, and to allow for the axial variation of dose due to the axial neutron flux variation, a factor $\bar{\Phi}$ is required in the two integral terms. These terms are integrated using the generalized trapezoidal approximation. The finite difference form thus becomes:

$$\frac{\partial^2 y(z,t)}{\partial z^2} = M(z,t) \left\{ \frac{1}{EI} + \frac{\bar{\Phi}\beta(1-\lambda)\Delta t_r}{I} \right\} + \frac{\bar{\Phi}\beta}{I} \sum_{i=1}^{r} \{\lambda \Delta t_i + (1-\lambda)\Delta t_{i-1}\}\, M(z,t')$$

$$- \frac{1}{a} \sum_{i=1}^{r} \{\mu\, \dot{S}_1(z,t') + (1-\mu)\, \dot{S}_1(z,t)\}\, \bar{\Phi} \Delta t_i - \frac{\alpha_{th}}{a} T_1(z,t) + \frac{d^2 y_o(z)}{dz^2} \tag{12}$$

where $t' = t - \Delta t_r$, and μ and λ take values between 0 and 1.

It is convenient to write the bending moment as:

$$M = \sum_{j=1}^{r-1} Q_j \ell_j + Q_r z \tag{13}$$

where Q_j is the shear force in the jth span, and z is read from the upstream end of each span.

As in IAMBIC, T_1 is the first harmonic component of the six clad temperatures calculated by the thermal/hydraulic routine at each calculation step for each pin and approximated in each span by a polynomial function. After each time increment T_1 is assumed initially to be the converged value from the previous step, but it is up-dated together with the values of Q_r by iteration between the pin bending equation and the thermal hydraulic equations. The converged values of Q_r are carried forward in the summation term.

A difficulty arises in dealing with $\dot{S}_1$. This quantity is the first harmonic component of the azimuthal variation of the instantaneous rate of swelling with dose. Although expressions are available for voidage growth as a function of dose and temperature they usually relate to data derived either at constant temperature or with a single step change of temperature, whereas in the pin bowing problem the temperature is changing continuously as bowing occurs. There is evidence to support the view that after some threshold dose the clad may have a memory for its early irradiation temperature and accumulate voids at a rate corresponding to that temperature regardless of any change [24]. However, it seems unlikely that the memory would persist to high dose. Two approaches are suggested which can readily be combined; the swelling rate at the current neutron dose and temperature equals the isothermal rate a) for that dose and temperature or b) for that dose and the initial temperature - the 'memory' effect.

For case (a) six values of $(\partial\epsilon_{sw}/\partial t)_T$ for the six sector clad temperatures at the current dose are read from appropriate swelling rules and the first harmonic components $\dot{S}_1$ for the x and y directions are calculated at each axial step.

For case (b) the integral is given by the first harmonic component of the aximuthal variation of the swelling strain at the current dose and the initial (converged) temperatures.

In each case a polynomial is fitted for each span and up-dated at each iteration, and the values at convergence carried forward for the next time step. The pin distortions follow straightforwardly by twice integrating eq. (12) and inserting the boundary conditions of specified or randomly selected grid cell mis-alignments, continuity of slope and overall force balance, $\sum_1^S Q_j = 0$. The new axial variation of sub-channel areas is then calculated, from which the new coolant flow distribution is obtained, enabling a re-calculation of clad temperature distribution to be made using eq. (1) and (3). New values of T_1 and $\dot{S}_1$ are calculated and used in eq. (12) to re-evaluate the pin distortions. The iterative cycle continues until convergence is achieved for that time step, or pins have bowed enough to touch. Convergence is assumed when the proportional changes in the values of shear force and slope at the upstream grid for each span and pin are sufficiently small. An abbreviated flow diagram showing the sequence of calculations followed in the TRIAMBIC code is given in Fig 3.

4. APPLICATIONS

In the case of a material having a 'memory' it is readily shown that the swelling integral in eq. (11) is approximately equal to the rate of change of swelling with temperature at constant dose multiplied by the transverse pin temperature gradient, ie $\alpha_{sw}\, T_1/a$. This

pseudo-expansion term cannot simply be added to the differential thermal expansion term, because the latter produces feed-back, whereas for a material with a memory the former does not. To assume feed-back of the induced clad temperature changes to the neutron voidage growth implies irradiation to the specified dose at the final temperatures, which is grossly pessimistic. However, the extremes of a) no feed-back from either term and b) feed-back from both terms will presumably bracket the correct solution. The IAMBIC code can be used in this way since case (a) corresponds to the first iteration and case (b) to the converged solution.

For some time the IAMBIC code has been used in this fashion to evaluate UK designs at specified neutron doses. The steady-state code cannot, of course, include the effect of creep, but since irradiation creep strength changes little from span to span the effect on the bowed shape is likely to be small.

Fig 4 shows radiographs of three fuel pins extracted from a sub-assembly irradiated in DFR to a dose of approximately 60 dpa. The central pin is quite straight, but some slight multiple bow is evident on the pin from the next edge row whilst severe multi-bow corresponding to grid frequency occurs on the peripheral pin as well as an overall simple bow. These patterns are consistent with differential neutron voidage bowing under the influence of cross-pin temperature gradients which thermal-hydraulic calculations predicted to be negligible for the centre pins, slight for the next row and severe for the edge pins. Also shown is the restrained shape of a peripheral pin as calculated by IAMBIC using pseudo-expansion coefficients. The calculated bow is smaller than is indicated by the radiographs even at the upper bound of the swelling rules. The induced temperature gradients are too small for feed-back to be significant.

Fig 5 shows how the maximum bow in a 37-pin cluster with typical LMFBR parameters (including over-cooling at the periphery) increases with neutron dose using 'best estimate' swelling values. The grid spacing is non-uniform and designed to minimise neutron voidage bowing. For initially straight pins the maximum calculated bow was less than 20% of the nominal pin-to-pin gap and there was no significant difference between cases assuming no feed-back and cases taken through several iterations. If the grid cells have positional errors of 0.075 mm (one standard deviation) then the maximum bow increases to 0.5 mm at 100 dpa but limiting clad temperatures are not exceeded. If upper bound swelling estimates are used IAMBIC predicts pin contact above a dose of 50 dpa.

Fig 6 is a typical graphical output from IAMBIC showing the x and y components of bow for a selected pin at high neutron dose.

5. CONCLUDING REMARKS

Whilst we appear to be some way off an all-embracing analytical method for thermal and neutron voidage bowing stability of fuel pins, considerable advances in understanding have been made. Further comparisons are needed between results from the various approaches to evaluate the validity and significance of the underlying assumptions, particularly in relation to creep effects in the bowing model, and flow distribution, heat transfer and mixing in the thermal-hydraulics model. Uncertainty of swelling and irradiation creep data remains a major problem.

The present work has highlighted the difficulty of application of swelling rules derived from isothermal tests to a situation of gradually changing temperature.

Application of the methods described here to typical LMFBR designs shows that a pattern of grid spacing related to the lengthwise distribution of curvature due to differential neutron voidage growth minimises the number of grids for a given maximum bow. It can also be arranged that the maximum bow occurs near the cooler end of the pin where a clad temperature well in excess of the nominal value of that point will fall far short of the design limiting value.

There is a case for irradiation experiments with pins pre-bowed into contact at various axial locations to assess the importance of pin bowing in relation to endurance.

6. ACKNOWLEDGEMENT

The writer is grateful to Dr T N Marsham, Managing Director, Northern Division, for permission to publish this paper. He would also like to acknowledge his indebtedness to his colleague Mr B D Williams for his invaluable assistance and considerable skill in coding the computer programs.

REFERENCES

[1] CAWTHORN, C, and FULTON, E J. Voids in irradiated stainless steel. Nature, 216, p.575, 11 November 1967

[2] BAGLEY, K Q, and others. Voids formed by irradiation of reactor materials. BNES Conference, Reading, March 1971

[3] GOSMAN, A D, and others. The SABRE code for prediction of coolant flows and temperatures. Paper 82, Int. Meeting on Reactor Heat Transfer, Karlsruhe, 1973

[4] ROWE, D S. COBRA-III: a digital computer program for thermal hydraulic analysis of rod bundle nuclear fuel elements. BNWL-B-82

[5] SHA, W T, and others. Boundary-value thermal hydraulic solution in a reactor fuel bundle. Nucl. Sci. and Engng, 59, No 2, February 1976

[6] BLOEMEN, H A, and others. The BOBL code: experimental verification of the hydraulic model. Netherlands Energy Research Foundation, ECN-9, December 1976

[7] VAN DER PUTTEN, A P W M, and others. On fuel pin bowing under LMFBR conditions. ANS Topical Meeting on Fast Reactor Safety, Beverley Hills, California, April 1974

[8] SUTHERLAND, W H, and WATWOOD, V B Jr. Creep analysis of statically indeterminate beams. BNWL-1362

[9] VEEDER, J, and SCHANKULA, M H. Bowing of pelletized fuel elements. Paper D1/6, 2nd SMiRT Conference, Berlin, September 1973

[10] MERCKX, K R. Computational procedure for the bowing of reactor fuel rods. Paper D1/6, 3rd SMiRT Conference, London, September 1975

[11] CORNET, G, and CAPART, G. Bowing stability of the peripheral pins in fast reactor sub-assemblies. Paper D1/8, 3rd SMiRT Conference, London, September 1975

[12] McAREAVEY, G. Thermal bowing of pins in fuel element clusters. Paper D1/7, 3rd SMiRT Conference, London, September 1975

[13] BETTS, C, and others. DFR 77-pin sub-assembly flow evaluation. UKAEA, TRG Report 644(R), 1963

[14] LYALL, H G. Measurement of flow distribution and secondary flow in ducts. CEGB, RD/B/N 1407, 1969

[15] LORENZ, J J, and GINSBERG, T. Coolant mixing and sub-channel velocity in an LMFBR fuel assembly. Nucl. Engng. and Design, 40, No 2, February 1977

[16] DWYER, O E, and others. Heat transfer to mercury flowing in line through an unbaffled rod bundle. Nucl. Sci. and Engng, 41, p321, 1970

[17] HOFMANN, F. The effect of geometric eccentricity upon axial and azimuthal temperature distributions in coolant cladding and fuel for sodium-cooled rod bundles. Progress in Heat and Mass Transfer, Vol 7. Pergaman Press, 1973

[18] PFANN, J. Turbulent heat transfer to longitudinal flow through a triangular array of circular rods. Nucl. Engng and Designs, 34, p.203, 1975

[19] MARCHESE, A R. Experimental study of heat transfer to NaK flowing in line through tightly packed rod bundles. Atomics International, TID-26896, October 1971

[20] ZHUKOV, A V, and others. Experimental study of the temperature fields of fuel elements using models. NASA Tech Trans, NASA-TT-F-522, May 1969

[21] NIJSING, R, and EIFLER, W. Temperature fields in liquid-metal-cooled rod assemblies. Progress in Heat and Mass Transfer, Vol 7. Pergaman Press, 1973

[22] ZHUKOV, A V, and others. Heat transfer from loosely spaced fuel rod clusters to liquid metal. NASA Tech Trans, NASA TT-F-522, May 1969

[23] HARRIES, D R. Irradiation creep in non-fissile metals and alloys. J. Nucl. Materials, 65, March 1977

[24] UKAEA internal document

NOMENCLATURE

a	outer radius of clad	α_{th}	coefficient of thermal expansion of clad
b	pin-to-pin gap	α_{sw}	pseudo-expansion coefficient
C_p	coolant specific heat	β	irradiation creep parameter
E	Young's modulus of clad	$\dot{\epsilon}$	strain
h	heat transfer coefficient	ζ	distance from neutral axis
I	2nd moment of area of clad	σ	stress
k	conductivity	Φ	relative neutron dose at z
k_e	'effective' conductivity of coolant	ϕ	relative pin power factor
ℓ	span length	Subscripts	
M	bending moment	c	(a) creep, (b) coolant
m	axial mass flow	e	elastic
N	number of adjacent sub-channels	i	ith time step
p	pin pitch	j	(a) span number, (b) adjacent sub-channel
Q	shear force	o	initial condition
q	linear heat rating	r	span number
S	total number of spans	s	clad
S_n	nth harmonic of swelling strain	in	start of calculation step
T	temperature		
T_n	nth harmonic of temperature		
t,t'	time, clad thickness		
w	transverse coolant flow		
x	component of pin deflection at z		
y	component of pin deflection at z		
z	axial distance		

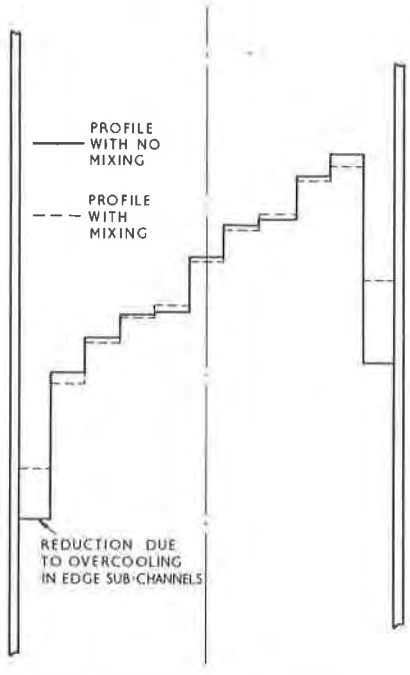

Fig. 1 Coolant temperature distribution across a sub-assembly

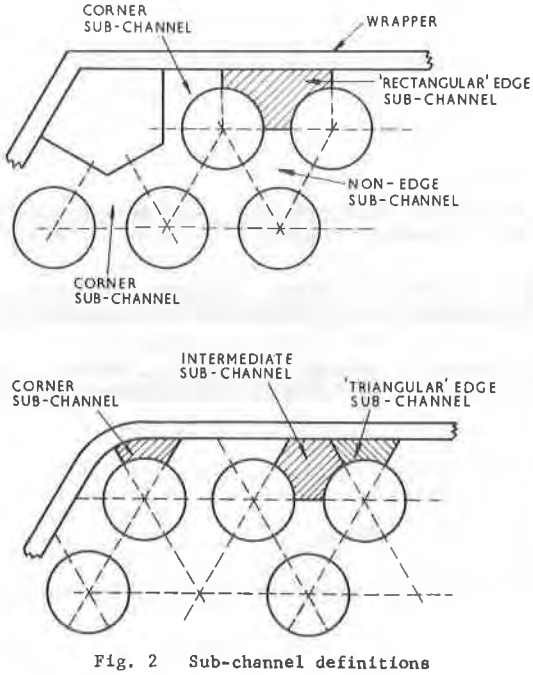

Fig. 2 Sub-channel definitions

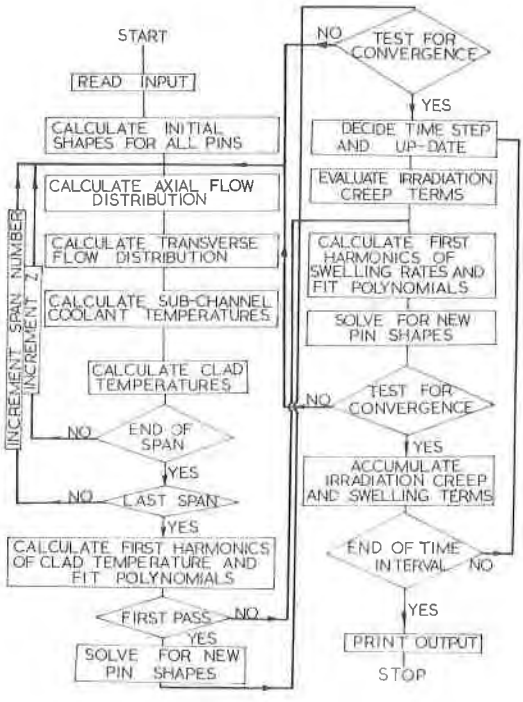

Fig. 3 Sequence of calculations in TRIAMBIC

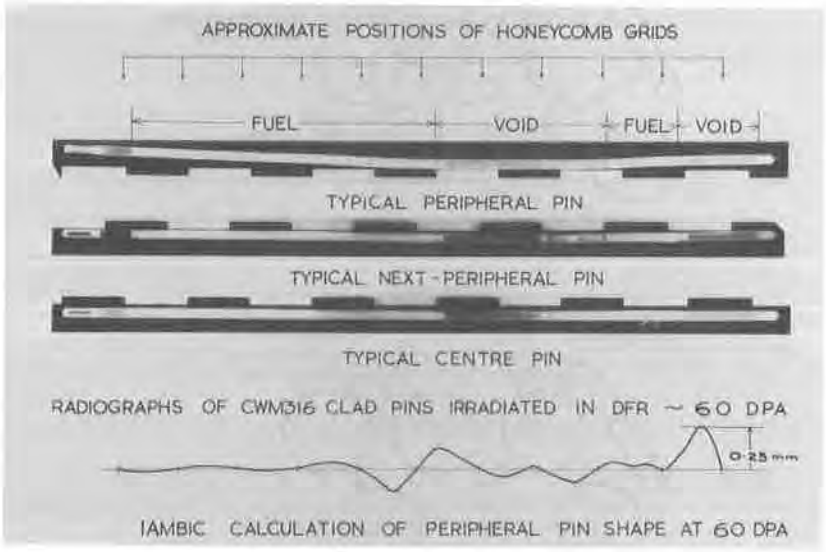

Fig. 4 Fuel pin distortions at high neutron dose

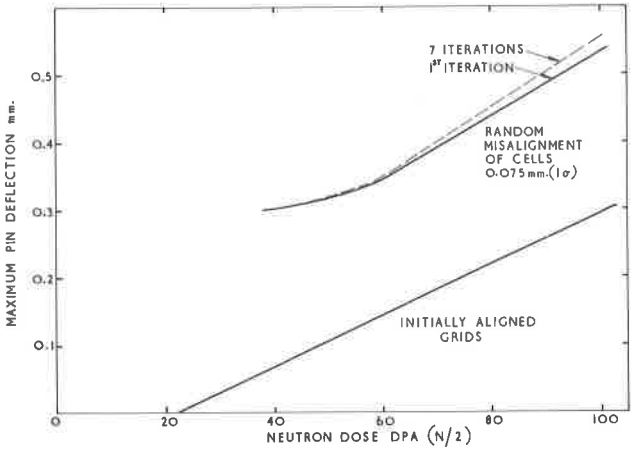

Fig. 5 Neutron voidage bow of peripheral pins in a typical LMFBR

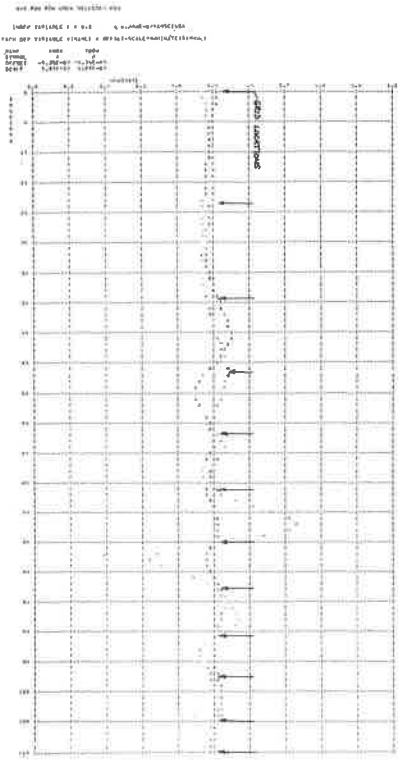

Fig. 6 Graphical output from IAMBIC for neutron voidage bowing of a typical LMFBR peripheral pin